Space Flight Enhances Autophagy-like Behavior in Human Neural Stem Cells

Nicholas Carpo , Victoria Tran , Juan Carlos Biancotti , Carlos Cepeda , Araceli Espinosa-Jeffrey *

Posted Date: 24 November 2023

doi: 10.20944/preprints202311.1529.v1

Keywords: microgravity; space flight; human neural stem cells; autophagy; intracranial hypertension

Article

Space Flight Enhances Autophagy-like Behavior in Human Neural Stem Cells

Nicholas Carpo [1], Victoria Tran [2], Juan Carlos Biancotti [2], Carlos Cepeda [1] and Araceli Espinosa-Jeffrey [1,*]

[1] Department of Psychiatry, UCLA, Los Angeles, CA 90095, USA; npgcarpo@gmail.com (N.C.); ccepeda@mednet.ucla.edu (C.C.)

[2] Department of Surgery, Division of Pediatric Surgery, School of Medicine, Johns Hopkins University, Baltimore, MD 21205; victoriakimtran@gmail.com (V.T.); jbianco5@jh.edu (J.C.B.)

* Correspondence: araceli@ucla.edu; Tel.: +1-310-825-1747

Abstract: Mammalian cells have evolved to function under Earth's gravity, but how they respond to microgravity remains largely unknown. Neural stem cells (NSCs) are essential for the maintenance of central nervous system (CNS) functions during development and the regeneration of all CNS cell populations. Here, we examined the behavior of space (SPC)-flown NSCs as they readapted to Earth's gravity. We found that most of these cells survived the space flight and self-renewed. Yet, some showed autophagy-like behaviors (ALB). To ascertain if the secretome from SPC-flown NSCs contained molecules inducing this behavior, we incubated naïve, non-starved NSCs in a medium containing SPC-NSCs secretome. We found a four-fold increase in the ALB rate. Proteomic analysis of the secretome revealed that the protein of highest content produced by SPC-NSCs was secreted protein acidic and rich in cysteine (SPARC), which triggers endoplasmic reticulum (ER) stress leading to lethal ALB. These results offer novel knowledge on the response of neural cells, particularly NSCs, subjected to space microgravity. Moreover, some secreted proteins have been identified as microgravity sensing, paving a new venue for future research aiming at targeting SPARC metabolism. Although we did not establish a direct relationship between ALB and SPARC as a potential marker, these results represent the first step in the identification of gravity sensing molecules as targets to be modulated and to design effective countermeasures to mitigate intracranial hypertension in astronauts using structure-based-protein design.

Keywords: microgravity; space flight; human neural stem cells; autophagy; intracranial hypertension

1. Introduction

After space flight, health anomalies, such as intracranial hypertension, flattening of the rear of the eyeball, bulging of the optic nerve, and other anatomical and systemic alterations such as white matter microstructural changes have been reported [1,2]. Therefore, microgravity-induced intracranial hypertension represents a risk factor, and it could become a potential limitation for long-duration space missions. Neural stem cells (NSCs) are crucial in the central nervous system (CNS) because they generate various cell types during development, and they maintain the integrity and function of the CNS in health and disease. Previously, we demonstrated that, just like in simulated microgravity, space microgravity (SPC-μG) induces enhanced proliferation of NSCs. We corroborated this during space flight [3] and confirmed that NSCs proliferated more than ground controls after space flight [4]. We also found that the vast majority of these cells adapted to Earth's gravity and displayed typical features of NSCs, such as self-renewal via normal proliferation, where cytokinesis occurred within the range of ground control cells without significant differences [4]. In this study, we examined the behavior of space-flown NSCs as they were adapting to Earth's gravity in more detail and found that some of the SPC-flown NSCs and their progenies displayed autophagy related events. For the purpose of this paper we named this phenomenon "autophagy-like behavior" (ALB). This phenomenon is reminiscent of what occurs during the development of the CNS. Nonetheless, it also plays a role in cell survival and cell death [5]. To examine if the secretome from SPC-flown NSCs contained a molecule(s) that would induce ALB, we cultured naïve NSCs in non-

 doi:10.20944/preprints202311.1529.v1

starving conditions using fresh NSCs growth medium containing the secretome produced by NSCs flown to space. There was a four-fold increase in ALB rate compared to non-treated naïve NSCs, raising the imminent need to analyze the secretome contents of SPC-flown cells to start unraveling what had enhanced this behavior. We report that the protein with the highest content was SPARC. This protein has been attributed numerous functions, it modulates the endothelial barrier function [6], it is constitutively expressed by proliferative human cerebral microvascular endothelial cells (hCMEC/D3) and its expression declines as these cells mature [6]. The encoded protein is required for collagen in the bone to become calcified. It is also involved in extracellular matrix synthesis [7] and induces cellular morphological changes. Among its pleiotropic functions, autophagy supports cell survival as well as cell death in different cells, organs, and conditions [8,9].

Altogether, our work uncovers the response of human neural cells, particularly NSCs, to the gravitational regulation of several stress related proteins. Moreover, it reveals an important phenomenon of the memory pool wherein some daughter NSCs born to SPC-flown ones display ALB on Earth's gravity. These novel features would not be possible to find in studies performed solely on Earth's gravity because SPARC is upregulated by space microgravity. Moreover, this study is significant to astronauts' health because it may be enhanced as a mechanism to compensate for the increased number of NSCs produced during and after space flight [3,4], which may induce a limited expansion of the astronauts' total brain size.

2. Materials and Methods

2.1. Cells and Culture System

Human tissue experiments were approved by the Office of the Human Subject Committee. Cultures were prepared with fetal human tissue specimens donated by the Department of Pathology and Laboratory of Medicine at the University of California, Los Angeles (UCLA). Samples were de-identified in accordance with National Institutes of Health (NIH) guidelines. Anonymous, preserved specimens are donated for medical research purposes and are Institutional review board (IRB) exempt (www.pathology.ucla.edu/TPCL.html).

2.2. Cultures of NSCs

A homogeneous population of NSCs was obtained from human induced pluripotent stem cells (hiPS). The original cells, known as "CS83iCTR-33n1" (such as skin cells), were "reprogrammed" and provided to us by Cedars-Sinai Medical Center via a material transfer agreement. We then induced these hiPS to the neural phenotype using our stem cell medium (STM). For detailed information on the culture medium and cell preparation, see previous work [10–12].

2.3. Space Flight

The BioScience-4 mission was launched onboard the Space-X 16 Dragon capsule on November 5th, 2018, being to the best of our knowledge the first study to investigate the proliferation of human CNS stem cells in space microgravity. This study has been instrumental to better understand features of neural cells while in space, as well as after returning to Earth [3,13]. For space flight, NSCs were seeded onto passive 8-well Petri dishes (Yuri), then flown to the ISS and installed in the Space Technology and Advanced Research System Experiment Facility-1 (STARS-F1, STaARS) at 37ºC. Cells remained onboard the International Space Station (ISS) for 39.3 days and then returned to Earth.

2.4. Recovery of the Hardware and Harvesting of Samples

After splashdown, samples were transported in a controlled environment from Long Beach airport to UCLA. The secretome was recovered from each well separately. Subsequently, NSCs were detached from the floors and walls of each well and recovered separately. Secretome samples were frozen for further use. Next, NSCs that were attached to the mesh carrier, were retrieved from the hardware, plated onto poly-d-lysine coated flasks in STM [10] and allowed to recover from space

Preprints (www.preprints.org) | NOT PEER-REVIEWED | Posted: 24 November 2023 doi:10.20944/preprints202311.1529.v1

flight. After 20 h in the incubator (5% CO2 and at 36.8°˚C), flasks were placed in a Zeiss Axio Observer 7 to visualize cells as they were adapting to terrestrial gravity (Figure 1).

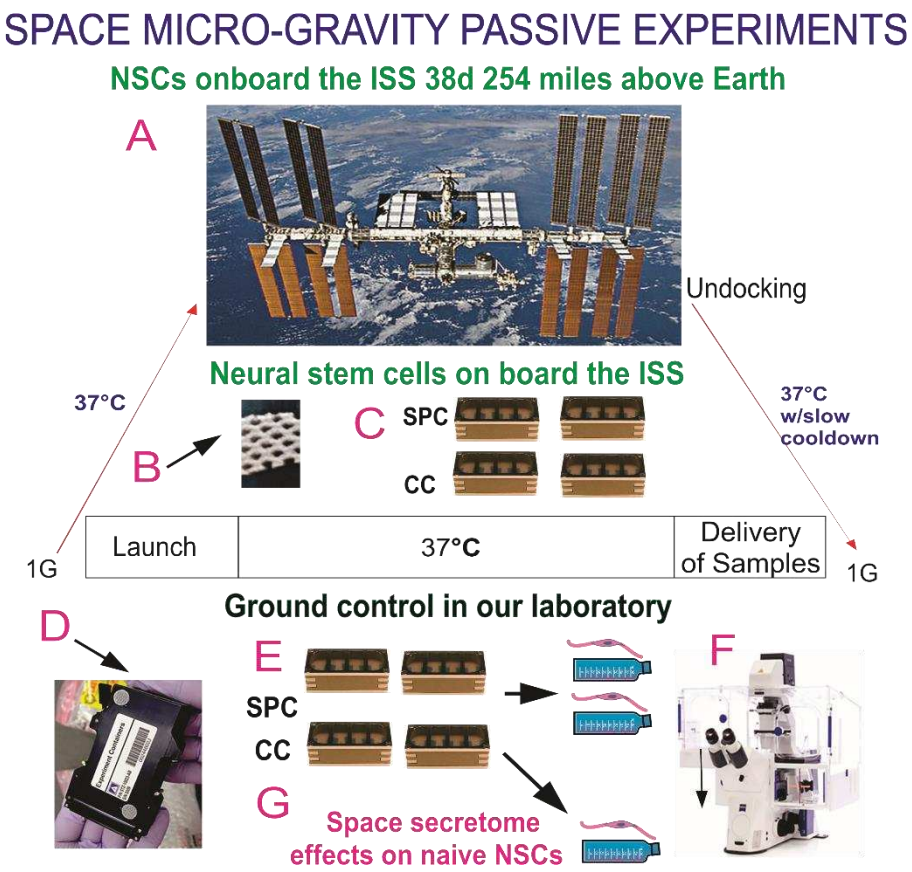

Figure 1. Synopsis of Passive experiments. Human neural stem cells (hNSCs), as part of the Bioscience-4 Space Biology NASA experiment, flown to the International Space Station (ISS) on board SpaceX-16 (A). It was launched on November 5, 2018 and landed (splash-down) on January 15, 2019. (a) ISS. The cells remained in microgravity for 39.3 days. Its orbit height was 254 miles; its speed on orbit was 4.76 miles/s; and maximal speed reached 17,400 mph. On Earth, humans are exposed to 3 to 4 millisieverts (mSv) of radiation from natural sources, per year, mainly from cosmic rays that make it through the atmosphere. On the ISS, astronauts receive about 150 mGV per six months. For the current mission, the average daily total radiation dose was 0.425 mGv on board the space station. This experiment is called "passive" because it was designed to mimic the trajectory astronauts' brains undergo during space flight (i.e., launch, stay in space, and splash down when returning to Earth) without manipulation or medium change; (b) Example of mesh carrier without cells. NSCs were seeded on the floating mesh carriers; (c) View of the 8-well Petri dishes used for the passive experiments on Earth. 4 chambers were used per condition; all chambers had an air permeable window; (d) External cover in which 8-well chambers traveled; (e) View of the external shell in which the units travelled and stayed while in space. The same number of chambers were flown to space and left on Earth in our laboratory as ground control. All cells were maintained at 37°C. Ground control cells were seeded in similar containers and maintained at the same temperature and conditions in our laboratory; the only difference between the set of NSCs flown to the ISS and the ground control set that remained in our laboratory was that the former was subjected to microgravity during space flight while the latter was subjected to only gravity; (F) Upon splashdown, the NSCs that were flown to the ISS were transferred from Kennedy Space Center to World Carrier and brought to Long Beach CA. The payload developer brought them to our laboratory (UCLA) at 37°C. Cells were recovered seeded and fed with fresh medium for time-lapse studies; (G) The secretome was collected from each well separately.

 doi:10.20944/preprints202311.1529.v1

2.5. Time-lapse Microscopy

We used the Zeiss Axio Observer 7 fully motorized inverted research microscope with the Zeiss Axiocam 506 monochrome camera with Zeiss ZEN software and definite focus equipped with the full Incubation XL chamber (Zeiss) for temperature control and with a motorized scanning stage. Images are displayed at 4 frames per second, where frames represent image captures taken 10 min apart.

2.6. Cell counts and Statistical Analysis

Statistical analyses were performed using One-Way ANOVA, followed by Tukey post hoc test in which $p<0.05$ was defined as statistically significant. For cell proliferation, we used Student's t-test, in which $p<0.05$ was defined as statistically significant. Statistics data are presented as mean ± SD.

2.7. Secretome collection and Proteomics Analysis

We used an automated hardware (Yuri) that allowed us to collect the medium produced solely in space during 26 h as previously described [12]. A synopsis of the experiment is shown in Figure S1. The culture medium that fed the cells during space flight was recovered from the hardware separately, medium from the cell chamber, and from each tank were placed in numbered tubes with addition of proteases inhibitor cocktail, and saved frozen at -80°C. For the purpose of this paper, we named this conditioned medium "secretome."

2.7.1. 2-D DIGE Preparation of samples

The conditioned medium samples (secretome) were thawed and vortexed for 20 s. The samples were spun for 30 min at 4°C at 14,000 rpm and the supernatant was collected. For these samples, serum Albumin and IgG were removed using Thermo Scientific Albumin/IgG Removal Kit. Next, the depleted serum samples were concentrated and exchanged into 2D Lysis buffer (Sigma Millipore, St. Louis, MO, USA) (7 M urea, 2 M thiourea, 4% CHAPS, and 30 mM Tris-HCl, pH 8.5). Protein concentration was measured in all samples using the Bio-Rad protein assay method. The Gel layout, Internal Standard (Cy2), space (0G) NSCs_0G (Cy3), ground control (1G) (Cy5) contained an equal amount of protein from each sample. CyDye labeling: For each sample, 30 μg of protein was mixed with 1.0 μL of diluted CyDye, and kept in dark on ice for 30 min. The labeling reaction was stopped by adding 1.0 μL of 10 mM lysine to each sample, and incubating in the dark on ice for an additional 15 min. The labeled samples were then mixed. The 2X 2D Sample buffer (8 M urea, 4% CHAPS, 20 mg/mL DTT, 2% pharmalytes, and trace amount of bromophenol blue), 100 μL destreak solution, and Rehydration buffer (7 M urea, 2 M thiourea, 4% CHAPS, 20 mg/mL DTT, 1% pharmalytes and trace amount of bromophenol blue) were added to the labeling mix to make the total volume of 250 μL. We mixed well and spun before loading the labeled samples into the strip holder.

2.7.2. Isoelectric focusing (IEF) and Sodium dodecyl-sulfate polyacrylamide gel electrophoresis (SDS-PAGE)

After loading the labeled samples, IEF (pH3-10 Non-Linear) was run following the protocol provided by GE Healthcare. Upon finishing the IEF, the immobilized pH gradient (IPG) strips were incubated in the freshly made equilibration buffer-1 (50 mM Tris-HCl, pH 8.8, containing 6 M urea, 30% glycerol, 2% SDS, trace amount of bromophenol blue and 10 mg/mL DTT) for 15 minutes with gentle shaking. Then the strips were rinsed in the freshly made equilibration buffer-2 (50 mM Tris-HCl, pH 8.8, containing 6 M urea, 30% glycerol, 2% SDS, trace amount of bromophenol blue and 45 mg/mL Iodoacetamide) for 10 min with gentle shaking. Next, the IPG strips were rinsed in the SDS-gel running buffer before transferring into 13.5% SDS-gels. The SDS-gels were run at 15°C until the dye front ran out of the gels.

 doi:10.20944/preprints202311.1529.v1

2.7.3. Image scan and Data analysis

Gel images were scanned immediately following the SDS-PAGE using Typhoon TRIO (GE Healthcare). The scanned images were then analyzed by Image Quant software (version 6.0, GE Healthcare), followed by in-gel analysis using DeCyder software (version 5.0, GE Healthcare). The fold change of the protein expression levels was obtained from in-gel, DeCyder analysis according to the DeCyder 2D Software User Manual 28-4010-06AB.

2.8. Protein Identification by Mass Spectrometry

2.8.1. Spot picking and Trypsin digestion

The spots of interest were picked up by Ettan Spot Picker (Amersham BioSciences) based on the in-gel analysis and spot picking design by DeCyder software. The gel spots were washed a few times then digested in-gel with modified porcine trypsin protease (Trypsin Gold, Promega). The digested tryptic peptides were desalted by Zip-tip C18 (Millipore). Peptides were eluted from the Zip-tip with 0.5 ul of matrix solution (α-cyano-4-hydroxycinnamic acid; 5 mg/mL in 50% acetonitrile, 0.1% trifluoroacetic acid, 25 mM ammonium bicarbonate) and spotted on the AB SCIEX Matrix assisted laser desorption/ionization (MALDI) plate (Opti-TOFTM 384 Well Insert).

2.8.2. Mass spectrometry

Matrix assisted laser desorption/ionization-time of flight mass spectrometry (MALDI-TOF MS) and TOF/TOF tandem MS/MS were performed on an AB SCIEX TOF/TOF™ 5800 System (AB SCIEX, Framingham, MA). MALDI-TOF mass spectra were acquired in reflector positive ion mode (as there is no requirement to confirm via negative mode). TOF/TOF tandem MS fragmentation spectra were acquired for each sample, averaging 4000 laser shots per fragmentation spectrum on each of the 10 most abundant ions present in each sample (excluding trypsin autolytic peptides and other known background ions).

2.8.3. Database search

Both resulting peptide mass and the associated fragmentation spectra were submitted to GPS Explorer workstation equipped with MASCOT search engine (Matrix Science) to search the database of National Center for Biotechnology Information non-redundant (NCBInr) or Swiss-Prot database.

Searches were performed without constraining protein molecular weight or isoelectric point, with variable carbamidomethylation of cysteine and oxidation of methionine residues, and with one missed cleavage also allowed in the search parameters. Candidates with either protein score C.I.% or Ion C.I.% greater than 95 were considered significant.

3. Results

3.1. Post-space flight observations of NSCs

In the current study, we were not able to visualize NSCs while in space due to the type of hardware chosen. Nonetheless, post-flight observations using time-lapse microscopy allowed us to follow their behavior and recovery in detail. After harvesting them from the 8-well flown hardware, NSCs were seeded onto T-75 flasks or flaskettes with glass bottoms for optimal quality imaging.

3.2. Space flight induces ALB in NSCs

After retrieving the cells from the flying devices, they were gently centrifuged and re-suspended in stem cell complete medium (STMc) and seeded onto poly-d-lysine coated flaskettes. Immediately after being seeded, they were placed in the time-lapse microscope system with an incubator to control temperature and the CO2 environment. We captured phase contrast images every 10 minutes to visualize the changes occurring in cells after space flight. We found that, compared to controls, a higher percentage of SPC-flown NSCs displayed ALB (Figures 2 and 3).

Preprints (www.preprints.org) | NOT PEER-REVIEWED | Posted: 24 November 2023 doi:10.20944/preprints202311.1529.v1

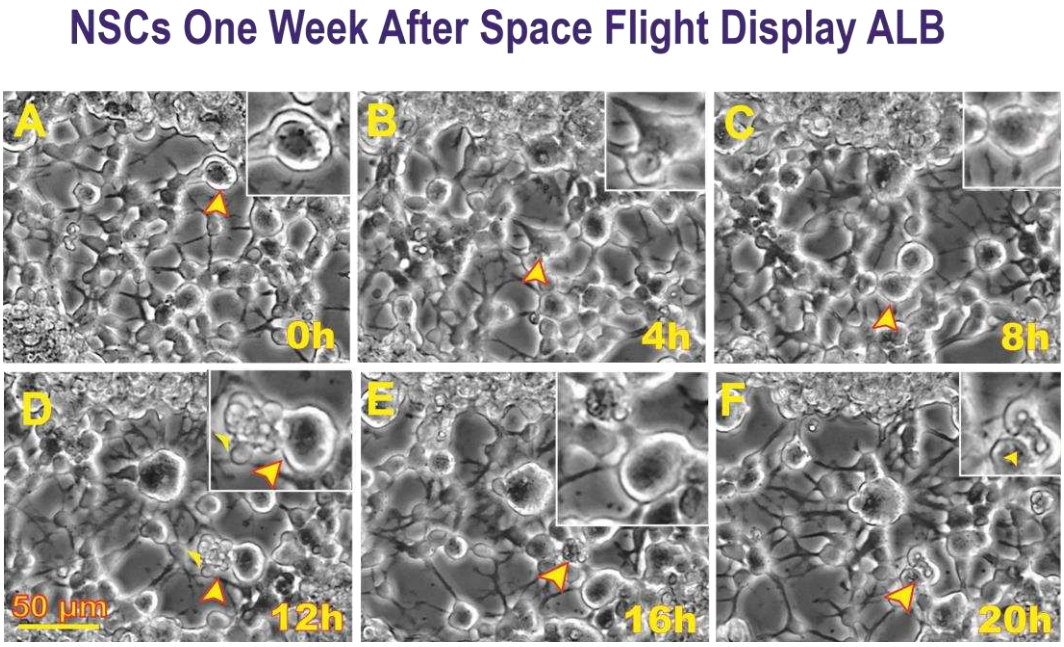

Figure 2. Human neural stem cells (NSCs) exhibited autophagy-like behavior (ALB) after space flight. Sequential views of the behavior of an NSC flown to space one week after returning to Earth. These views were analyzed as cells with ALB were counted and evaluated through tracking in reverse time. (A) Cell 13.25 h following initiation of the time-lapse capture; (B) The cell shows structural transformations as it appears to fuse with another NSC; (C) 8 h following the initial frame, the cell underwent morphological differences again and had not fused with its neighbor; (D) After 4 h, some cells contents were expelled; (E) After 4 h, the cell had internalized the contents which were previously expelled; (F) Then, a pocket-like formation formed through the contraction of the cell within 20 h. A video of this event is shown in Video S1.

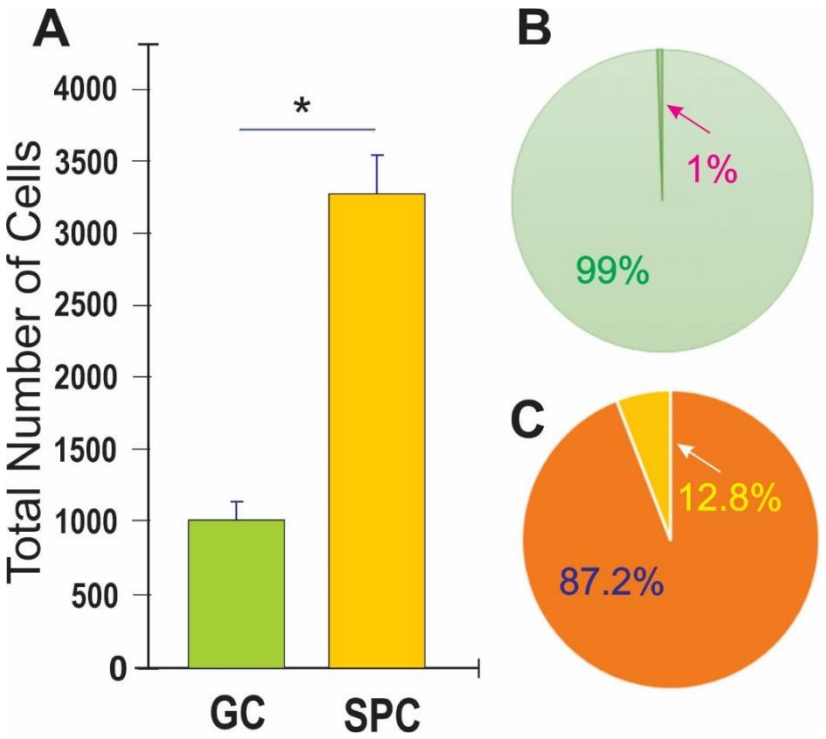

Figure 3. Human NSCs displayed enhanced ALB after space flight. (A) This bar graph shows the average of the total number of cells present 44h after the time-lapse started. The green bar denotes ground control (GC)-NSCs with no exposure to space microgravity (SPC-µG). The orange bar denotes

Preprints (www.preprints.org) | NOT PEER-REVIEWED | Posted: 24 November 2023 doi:10.20944/preprints202311.1529.v1

SPC-NSCs one-week post-flight; (B) Results shown as a percentage where only 1% of GC-NSCs exhibited ALB (green pie graph) as compared to the 12% SPC-NSCs showing ALB orange pie graph (C). Data analysis was performed with one-way ANOVA followed by the Tukey multiple comparisons test in which * $p<0.05$ was defined as statistically significant. Data represent the mean of four separate scenes for each color-coded condition.

3.3. SPC-flown NSCs' secretome increases naïve NSCs ALB

Having observed ALB in some of the NSCs back from space, we then sought to determine if naïve NSCs that had not been left unattended and were fed fresh culture medium prior to performing the experiment would respond to the secretome from SPC-flown NSCs by displaying autophagic behavior. Naïve NSCs were plated onto the flaskettes (flasks on slide) and left overnight in STMc. The next day, to make sure that cells were not starved, fresh STMc medium with SPC-secretome (2:1) was prepared to replace the medium in the culture to be imaged. Interestingly, upon exposure to the SPC-secretome, we observed the same phenomenon, displayed by SPC-NSCs and their progenies, in naïve NSCs. The response was gradual and increased with time after incubation in the SPC-secretome-supplemented culture medium (Figure 4). A video time-lapse of this event is shown in Video S2.

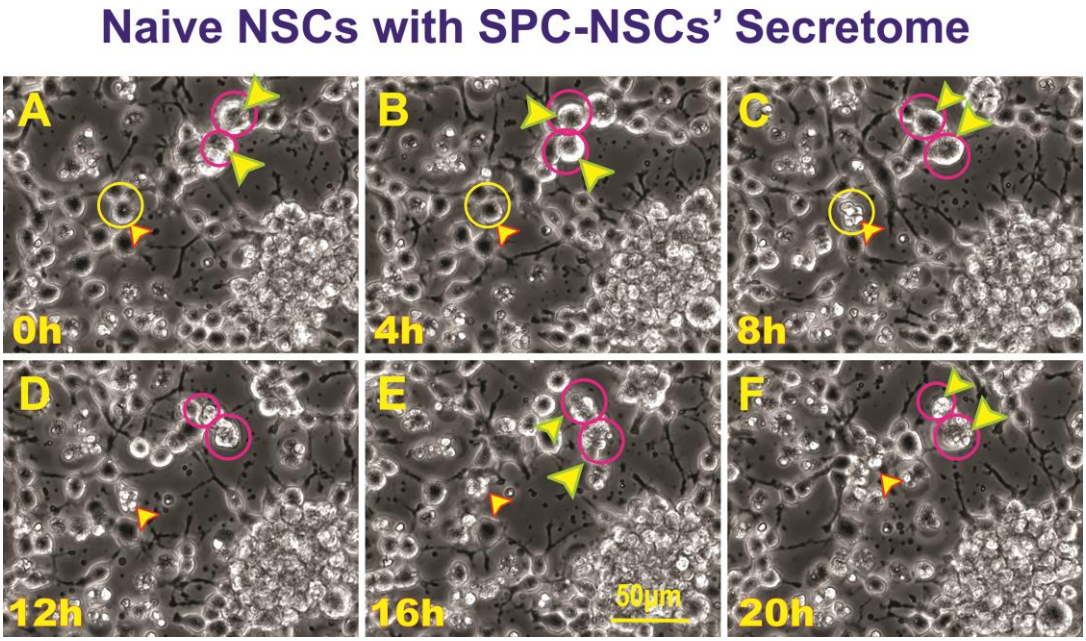

Figure 4. Unveiled effects of SPC-NSCs-secretome on enhanced ALB in Naïve NSCs. Sequential views of the behavior of naïve NSC incubated in a culture medium containing the secretome produced by NSCs flown to space. The cultures were examined to identify cells undergoing ALB. Once a cell was identified, it was then studied through reverse-time tracking. At the beginning of the time-lapse acquisition, the cells looked round and healthy. Note that at least three instances of ALB are observed in the field of view. (A) View of a cell being studied 13.25 h after the start of the time-lapse capture yellow circle and arrow, in the same field two larger cells labeled with red circles and arrows; (B) Morphological changes observed, the cell encircled in yellow looks healthy and still bearing cell processes. The two larger cells encircled in red look rounder and healthy as well; (C) 8 h after the time-lapse was started, the cell shown in the yellow circle had expelled material from its soma. The two cells inside red circles are less round and still look health; (D) In the lapse of four hours, the cell in the top red circle had deposited some of its contents onto the extracellular space while the one in the bottom circle looked ruffled; (E) 4 h later, the cell in the top red circle appears to have internalized the expelled material, while the cell below that one had become larger; (F) The cell then contracted until there was just a small pocket-like structure. The event was completed within the lapse of 20 h. Video time-lapse of this event is shown below (Video S3).

Preprints (www.preprints.org) | NOT PEER-REVIEWED | Posted: 24 November 2023 doi:10.20944/preprints202311.1529.v1

3.4. ALB also occurs in untreated, naïve NSCs although to a much lesser extent

Naïve NSCs were seeded in STMc and kept overnight. The next day, the medium was replaced with freshly prepared STMc medium, and the flaskette/flask on slide was placed in the time-lapse system. The starting time was considered time 0. As an illustration of ALB in naïve NSCs (Figure 5), at 8:20 h, a cell divided and continued moving in various directions. Eventually, the cell expelled intracellular material, re-captured it, and finally died. Therefore, by the 30th hour from the beginning of the time-lapse series, one cell underwent ALB while the second cell remained alive and migratory for the rest of the study.

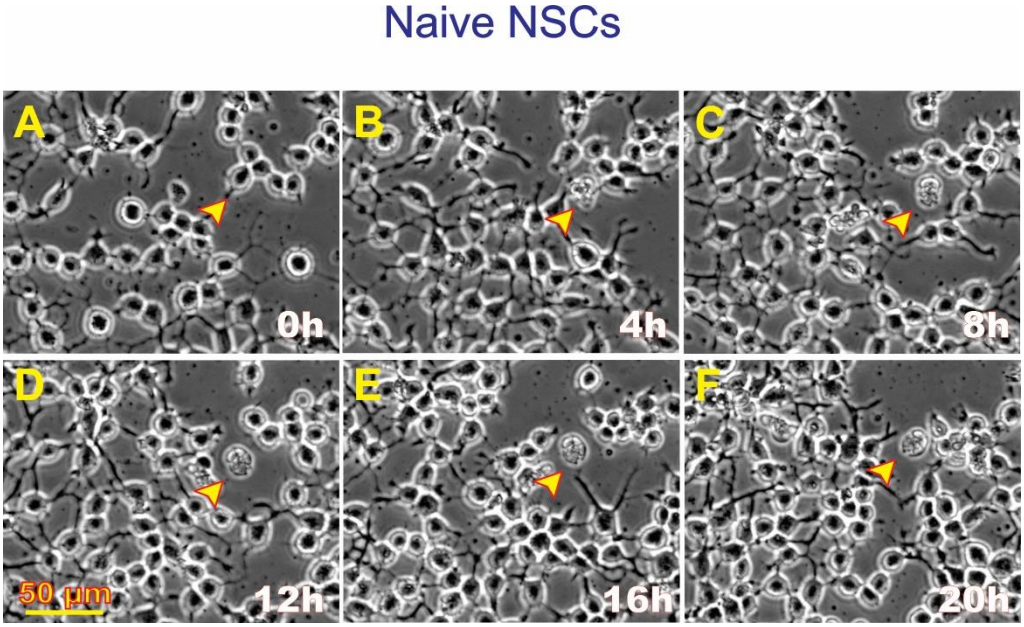

Figure 5. Example of ALB displayed by naïve NSCs. Compared with the naïve cultures incubated with the NSCs' secretome, it was extremely difficult to locate naïve NSCs presenting ALB in the absence of the space-derived secretome. (A) Shows a live cell with two cell processes; (B) Four hours later, the cell had excreted some material; (C) The cell remained attached to its material; (D) No major changes were observed; (E) There were no changes; (F) Only the debris was observed. This time-lapse sequence below shows the healthy status of the vast majority of Naïve NSCs where it was very difficult to find cells undergoing ALB. The process appears to have started between 0h and 4h after the time-lapse series had started. The cell remained virtually unchanged after that.

We then compared the frequency of ALB events in naïve NSCs cultured solely in the STM and naïve NSCs grown in a medium containing STM plus the secretome of SPC-flown NSCs (2:1 v/v). We found that ALB was upregulated in NSCs treated with the secretome of SPC-NSCs since the beginning of the treatment. Naïve NSCs alone had a very low incidence of ALB, no more than once during the first 12 h and no more than 8 to 10 up to 36 h. In contrast, cells with the SPC-secretome had their lowest frequency of ALB within the first 6 h. The incidence increased by ~5 more events for the next 12 h; 10 more events between 18 h and 24 h, and then it jumped to around 25 events within the following 6h (from 24 h to 30 h) up to 44 h while untreated naïve NSCs remained at a basal level as shown in Figure 6.

Preprints (www.preprints.org) | NOT PEER-REVIEWED | Posted: 24 November 2023 doi:10.20944/preprints202311.1529.v1

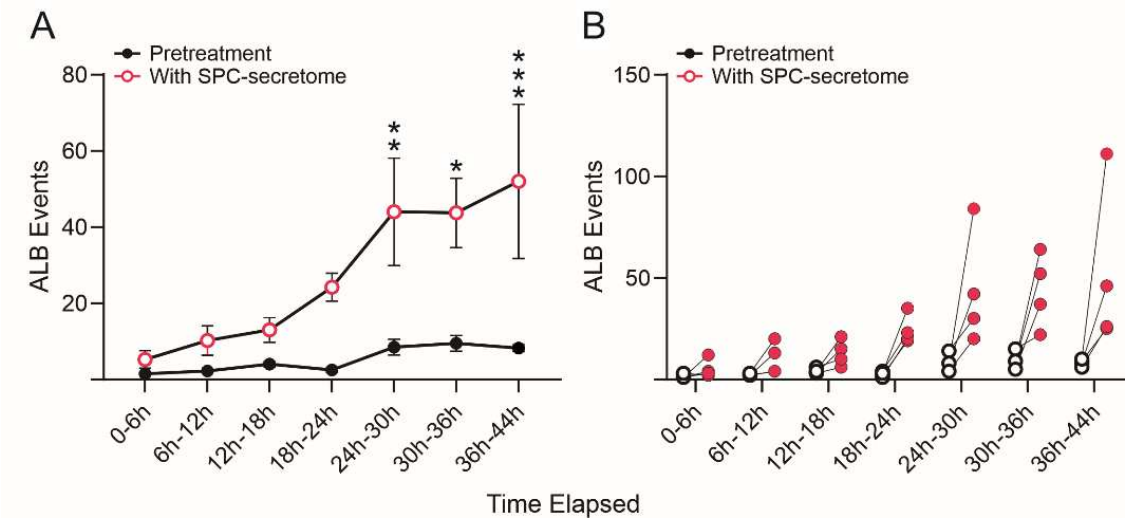

Figure 6. SPC-NSCs-produced secretome enhanced ALB in Naïve NSCs. Comparison of the number of ALB events in naïve NSCs in STM medium alone and naïve NSCs grown in medium containing STM + the secretome of SPC-flown NSCs (2:1 v/v). We found that ALB was upregulated in NSCs treated with the secretome of SPC-NSCs since the beginning of the treatment. Untreated naïve NSC cultures had a very low number of cells undergoing ALB starting with 1 to 2 cells in the first 12 h, increasing to an average of 5 to 9 cells until the end of the study 44 h later. (A) The graph represents the average number of events observed in the 4 samples examined before and after exposure to the secretome medium. (B) The graph shows individual changes in the number of ALB events before (black open dots) and after (red dots) changing to the secretome-containing medium. Statistical analysis was performed using Two-way Repeated Measures ANOVA and the interaction time x pretreatment x secretome was highly significant ($p=0.0065$, $F(6, 18) = 4.418$). Tukey's multiple comparisons post-hoc test demonstrated statistically significant increases at the 24-30 h ($p=0.0088$), 30-36 h ($p=0.0123$) and ($p=0.001$) bins.

To eliminate the possibility that the observed effects of the secretome were due to the fact that these cells were derived from hiPS, we next tested the SPC-NSCs' secretome on naïve non-starved OLPs derived from 18 weeks-human embryonic brain and we observed a deleterious effect on these OLPs, where they started to die within the first 5 h (Figure S2).

3.5. Secretome analysis

Proteomic analysis of SPC-flown NSCs' secretome revealed the enrichment of several proteins involved in stress-related pathways [14], and in particular, a subset of proteins associated to processes conducive to ALB. The most significantly enriched members are "Secreted Protein Acidic and Rich in Cysteine" (SPARC, 12.84), Calreticulin (CALR, 5.2), and Endoplasmin (ENPL, 3.3), members of the endoplasmic reticulum (ER) Stress Response pathway; Heat Shock Protein 90-beta (P90AB1, 7.3), Heat Shock Protein A8 (HSPA8, 3.7), and Vimentin (VIME, 2.1) implicated in the Chaperone-Mediated Autophagy and Late Endosomal Microautophagy (Table 1).

Table 1. Enrichment of the top-ranked proteins.

Space-flown NSC Proteomics			
SPC/1G	**Accession No.**	**Gene**	**Top Ranked Protein [Species]**
12.84	HUMAN	SPARC	SPARC OS=Homo Sapiens OX =9606 GN=SPARC PE=1 SV=1
7.3	HUMAN	P90AB1	Heat shock protein HSP 90-beta OS=Homo sapiens OX=9606 GN=HSP90AB1 PE=1 SV=4
5.2	HUMAN	CALR	Calreticulin OS=Homo sapiens OX=9606 GN=CALR PE=1 SV=1

 doi:10.20944/preprints202311.1529.v1

3.7	HUMAN	HSPA8	Heat shock cognate 71 kDa protein OS=Homo sapiens OX=9606 GN=HSPA8 PE=1 SV=1
3.3	HUMAN	ENPL	Endoplasmin OS=Homo sapiens OX=9606 GN=HSP90B1 PE=1 SV=1

4. Discussion

Before discussing our findings in more detail, a number of limitations have to be underlined. First, our definition of ALB does not exactly fit the canonical definition of autophagy, namely the formation of intracellular vacuoles and the degradation of intracellular substrates. Second, due to the nature of the study, experimental manipulations could not be easily performed while cells were subjected to microgravity, e.g., use of traditional autophagy markers such as LC-3. Thus, our evidence of ALB is indirect and limited to the effects observed while SPCs were readapting to earth's gravity or effects induced by the secretome of SPCs on control cells. Notwithstanding these limitations, our study provides new insights critical for the understanding of the effects of long-term space travel, inclucing the discovery of SPARC as a potential marker of microgravity-induced autophagy.

4.1. Microgravity as a potential modulator of ALB

The lysosomal catabolic degradation mechanism, known as autophagy, is essential to maintain cellular survival and function, and it is activated in situations of cellular stress [15,16]. Autophagy involves the sequestration of autophagosomes that fuse with lysosomes and lead to cellular degradation. It has two very critical roles in eukaryotic cells [17,18]; one is nutrient recycling, and the second is eliminating excessive or harmful cellular products such as protein aggregates, supramolecular structures, or organelles such as mitochondria or peroxisomes.

In the present study, one could argue that our cells flown into space may have been starved because they were unattended, and that the ALB observed was a direct consequence. Nonetheless, when ground control cells were grown on Earth's gravity in the same conditions, ALB remained within basal levels throughout the experiment. Moreover, the naïve NSCs were not deprived of nutrients at any point in time; and yet, those receiving fresh culture medium supplemented with the SPC-NSCs secretome displayed ALB from the beginning of the experiment and the frequency of events increased with time spent in contact with the space secretome. Thus, the secretome effect was much more potent than that of space flight. Since these cells responded to the secretome in 1G and without starvation, it is likely that this phenomenon was upregulated via one or more of the secreted proteins. Thus, SPARC appears to be a gravity sensor whose effects are potentiated by Earth's gravity and mitigated while in microgravity. Yet, instead of triggering an effect similar to that on SPC-flown NSCs and naïve NSCs, the SPC-flown secretome was very deleterious to OLPs derived from embryonic brain, indicating that OLPs are more vulnerable to the SPC-produced secretome than NSCs. Studies on pathways to cell death have shown that rapamycin induces starvation-like behaviors by blocking mTOR [19]. Chaperone-mediated autophagy was the first studied process indicating degradation of intracellular components by the lysosome. It is a selective autophagic pathway mediated by chaperones such as HSPA8 [20]. In contrast, late endosomal microautophagy is a non-selective autophagic pathway that involves internalization of cytosolic cargo through invagination of the lysosomal membrane. Microautophagy is coordinated and complements other forms of self-eating pathways, such as chaperone-mediated autophagy and macroautophagy, among others [21].

Considering this is a pioneer study, the scope of our grant did not include an in-depth molecular characterization because neither sample size nor funding would allow it. Nonetheless, space flight definitively exerts stress on mammalian cells and organisms, which most likely contributed to ALB described here.

 doi:10.20944/preprints202311.1529.v1

4.2. Microgravity as a modulator of ALB proteins

Space flight involves a plethora of stressful events for individuals and cells in culture. Examination of the secretome of NSCs after space flight showed an increase in SPARC, which is known to participate in extracellular matrix synthesis and remodeling as it intervenes in the morphological changes of cells. SPARC is also known to be present during embryonic and postnatal growth in radial glia cells, blood vessels, and structures originating from the pia [22]. The rostral migratory stream also displays this protein, and its sequential spatial restriction leads to its expression solely in the adult's brain sub-ventricular zone (SVZ). In specialized glial cells, SPARC expression is enhanced [22]. Exogenous SPARC stimulates cell growth in low serum correlating with metastatic behavior [23–26]. Plasmid-overexpressed SPARC also triggers stress of the ER and unfolded protein response (UPR). Interestingly, inhibition of ER stress leads to an inhibition of autophagy-mediated apoptosis. Thus, ER stress plays a critical role in the regulation of autophagy-mediated apoptosis in SPARC-overexpressing neuroblastoma cells and radiation therapy [27,28]. Taken together, these studies suggest that our NSCs that were grown in a culture medium without serum, in space may have acquired characteristics approaching those of cancerous cells insofar as they proliferated more than sister cultures grown on Earth [4]. In addition, its expression increases in models of glutamate excitotoxicity and when knocked down, reduces neuronal injury [29]. The same study showed that glutamate excitotoxicity involves autophagy. Upon glutamic acid stimulation, LC3II/LC3I increases resulting in autophagy activation [29]. Overexpression of SPARC induces apoptosis in medulloblastoma by triggering ER stress and UPR [28]; and in neuroprimitive neuroectodermal tumors (PNET) through different pathways [28,30,31].

Thus, SPARC modulation on Earth appears to be an appealing approach to arrest the growth of cancerous cells in several organs and cell types [29,32]. Nonetheless, it is possible that its aberrant elevated expression promoted by microgravity induced increased NSCs proliferation [4]. Moreover, as shown in the present study, it may be deleterious if left uncontrolled in the brain of astronauts embarking on long-term space travel such as to the Moon and Mars. Because SPARC plays many roles in the fate and physiology of cells, it is plausible that it is a target protein whose modulation will help maintain cellular homeostasis in the brain. Regulation and maintenance of healthy levels of SPARC and cell numbers in the CNS are of utmost importance for the success of long-term space missions. By suppressing the elevated expression of SPARC we may be able to reduce the excessive proliferation of NSCs that occurs in cases like that of melanoma cells where SPARC-acquired expression increases their survival by suppressing p53 and the subsequent inhibition of the apoptotic pathway [33]. More studies using microgravity will allow the characterization of all the proteins that might have contributed to the deleterious ALB in our cells.

4.3. Space flight and radiation during SpX-16

Among other potential contributing factors for the phenomena observed, is radiation. There are two sources of ionizing radiation onboard the ISS, galactic cosmic radiation (GCR) and trapped protons whose dose accumulates mainly during passages through the South Atlantic Anomaly (SAA). The instruments that took the data from the Space Radiation Analysis Group, Johnson Space Center (JSC-SRAG) use information on the ISS orbit combined with mapping of the geomagnetic field to break out the dose into GCR and SAA components. The actual radiation during the space mission is shown in Table 2.

Table 2. Radiation information for the space mission.

	Mission GCR Dose (mGy)	Mission SAA Dose (mGy)	Mission Total Dose (mGy)	Maximum Daily Total Dose (mGy)	Minimum Daily Total Dose (mGy)	Average Daily Total Dose (mGy)
SpX-16	5.197	8.022	13.219	0.417 (12/17/18)	0.322 (1/12/19)	0.357 (0.026)

 doi:10.20944/preprints202311.1529.v1

Although in the present manuscript we did not address the effects of radiation on NSCs while in space, the average dose of radiation is 0.3-0.4 mSv/day in ISS, where protons are the principal space radiation source in the ISS. Therefore, SPC-NSCs were exposed to some radiation adding to the stress of their ER.

Because autophagy affects cell proliferation and survival, reports have shown that modulation of autophagy can improve the outcome of cancer treatment in combination with radiotherapy [34]. For glioblastoma, the most aggressive brain cancer, Palumbo and collaborators [35] described a differential involvement of autophagy in two human malignant glioma cell lines undergoing combined irradiation and temozolomide treatments. In such a model, radiation-induced ER stress protein expression is linked to protein folding, UPR, and radiation-induced autophagy [36]. The suppression of autophagy is now accepted as an important cytoprotective mechanism that enhances the response of cancer cells to multiple treatments [37]. Lastly, it has been reported that TNFalpha produces a similar pattern of morphological changes including bleb-formation in their cytoplasmic membrane, shrinkage and death. Nonetheless, this type of cell death is not autophagy-related. In cases of inflammatory processes, blebbing of cell membranes occurs in order to phagocyte, clear, and prevent inflammatory/autoimmune response [38].

In our case, the therapeutic targeting of ALB in NSCs may be the key to mitigating intracranial hypertension in astronauts, and radiation deserves deeper investigation as a subject with the aim of producing combinatorial therapies for the successful future of space exploration.

In summary, here we report two novel findings: the increased secretion of ER stress related proteins SPARC, calreticulin and endoplasmin by space flight and the induction of ALB in NSCs detected after space flight. While the SPC-NSCs-produced secretome gave rise to the same effects on naïve NSCs, we have also observed a similar phenomenon produced by the secretome of SPC-flown OLPs [39]. Nonetheless, the different cell types that form the CNS and the vasculature, either alone or in concert may respond differently to microgravity. Therefore, it is important to examine proteogenic upregulation in the context of the entire brain during, prior to, and after space flight, where all the cell types interact and work in concert leaving the possibility that one cell type may prevent SPARC up-regulation and ALB.

One question that comes to mind is that while in space, the exposure to microgravity also implies exposure to radiation. We believe that this is a promising start that will allow us to address intracranial hypertension in astronauts, preventive measures for future astronauts flying to space as well as effective countermeasures for astronauts currently in the ISS and those that have preceded them.

Supplementary Materials: Figure S1: Spaceflight automated experiment, Figure S2: The Secretome of SPC-Flown Neural Stem Cells is deleterious to Naïve OLPs, Video S1: SPC-NSCs autophagy two weeks postflight; SPC-NSCs exhibited autophagy-like behavior (ALB) two weeks post-flight. This time-lapse sequence shows the conditions of the cells when the time-lapse capture started. They were arranged as single cells or clusters made-up of clonal cell proliferation. The cells look healthy and bear multiple cell processes. The yellow arrow shows a cell that slowly deteriorated and died by autophagic cell death. This mp4 video is displayed at 4 frames per second, where frames represent image captures taken 10 minutes apart. Video S2: View of Naïve NSCs with NSCs secretome; View of Naïve NSCs with SPC-flown NSCs secretome. This time-lapse sequence shows the condition of the cells when the time-lapse capture started. They all bore cell processes and were arranged as single cells or clusters made-up of clonal cell proliferation. The dynamics of an autophagy-like event wherein the cell was bipolar and in contact with two other cells held by each cell process, eventually the cell bore the morphology of a small dividing cell and held by opposite cells as trying to help it divide. Nonetheless it did not divide and excreted some material moving among neighboring cells and finally dying by the end of the timelapse. The culture aspect had changed enormously as many NSCs proliferated giving rise to more and larger clusters. This mp4 video is displayed at 4 frames per second, where frames represent image captures taken 10 minutes apart. Video S3: High magnification view of naïve human OLPs with NSCs secretome. View of naïve human Oligodendrocyte Progenitors (OLPs) with NSCs secretome. In order to test if the effects of SPC-NSCs secretome were cell-specific related, we added it to human OLPs that had not been exposed to microgravity. The majority of these cells, whether as clusters or as single cells, had become unhealthy with ruffle-like cytoplasmic membranes, most of them were devoid of cell processes, and their debris were visible on the surface of the flaskette. The arrow points to a cell that is located near unhealthy or dead cells. This particular cell, although unhealthy, still bore short processes nonetheless and at a given point collapsed depositing all its intracellular

material onto the substratum. (For details of the experiment, see main text). This mp4 video is displayed at 4 frames per second, where frames represent image captures taken 10 minutes apart. Reference [12] is cited in the Supplementary Materials.

Author Contributions: Conceptualization, A.E.-J.; methodology, J.B. and A.E.-J.; software, A.E.-J.; validation, N.C. and C.C; investigation, A.E.-J.; resources, A.E.-J.; data curation, N.C., V.T. and A.E.-J.; writing—original draft preparation, N.C. and A.E.-J.; writing—review and editing, N.C., C.C. and A.E.-J.; visualization, N.C. and A.E.-J.; project administration, A.E.-J.; funding acquisition, A.E.-J. All authors have read the manuscript and agreed to the published version of the manuscript.

Funding: This research was funded by NASA Space Biology Grant, grant number NNX15AB43G; the Cell Culture and Imaging Core is supported by the NIH (Grant U54HD08710).

Institutional Review Board Statement: Not applicable. The cell line was created in Cedars Sinai and we obtained vis MTA. Therefore, we did not need IRB because we did not work with the original fibroblasts.

Informed Consent Statement: Not applicable.

Data Availability Statement: The data presented in this study are available on request from the corresponding author.

Acknowledgments: We are very thankful to Dr. Amy Rowat and her research team, for allowing us to use their time-lapse microscope system on short notice at a crucial time to be able to capture the changes produced by Earth's gravity on neural stem cells after space flight. We are extremely grateful to Mark Mobilia and the entire Zeiss team who provided unconditional assistance for long-term time-lapse imaging of our cells flown onboard SpX-16. The advancement of science is based on fundamental discoveries that would not be possible without the adequate tools and the timely help from supportive people and the Zeiss team is the perfect example. Having a loaner Zeiss Axio Observer 7 allowed us to acquire quality data. We also thank Dr. Fathi Karouia, Amy Gresser. Elizabeth Pane, and Araceli (Medaya) Torres for their help with the logistics for the study. The NASA Space Biology Project team at Ames Research Center Dr. D. Tomko, K. Sato, E. Taylor, ARC Space Biology Project Manager and the support personnel at the Space Station Processing Facility at Kennedy Space Center. Without their help, the flight would not have been possible. Special thanks for space flight support to Maria Birlem and Chriss Bruderrek from Yuri and STaARS team members Heath Mills, Tom Kyler, Jacquelyn Schoppe and BreAnne MacKenzie, Uli Kuebler from Airbus Defense and Space who introduced us to their flying hardware. We thank the astronauts that helped with this study while onboard the ISS and Jack Miller for summarizing the dosimetry data during this mission. Thanks to Applied Biomics for theyr support. We also thank Dorwin Birt for help with computer and imaging systems. Thanks to Elida Escalante for the preparation of the mesh carriers and Aurora Espinosa de los Monteros for help editing the text. We thank Dr. Stephen Cederbaum and Harley Kornblum for his signature on the students' contract. Last but not least, we thank the late Dr. Jean de Vellis for his enthusiastic support of our pioneering studies on the effect of microgravity on neural cells.

Conflicts of Interest: The authors declare no conflict of interest.

References

1. Kramer, L.A.; Hasan, K.M.; Stenger, M.B.; Sargsyan, A.; Laurie, S.S.; Otto, C.; Ploutz-Snyder, R.J.; Marshall-Goebel, K.; Riascos, R. F.; Macias, B.R. Intracranial Effects of Microgravity: A Prospective Longitudinal MRI study. *Radiology* **2020**, *295*, 640–648. https://doi.org/10.1148/radiol.2020191413.
2. Lee, J.K.; Koppelmans, V.; Riascos, R.F.; Hasan, K.M.; Pasternak, O.; Mulavara, A.P.; Bloomberg, J.J.; Seidler, R.D. Spaceflight-Associated Brain White Matter Microstructural Changes and Intracranial Fluid Redistribution. *JAMA Neurology* **2019**, *76*, 412–419. https://doi.org/10.1001/jamaneurol.2018.4882.
3. Cepeda, C.; Vergnes, L.; Carpo, N.; Schibler, M.J.; Bentolila, L.A.; Karouia, F.; Espinosa-Jeffrey, A. Human Neural Stem Cells Flown into Space Proliferate and Generate Young Neurons. *Applied Sciences* **2019**, *9*, 4042. https://doi.org/10.3390/app9194042.
4. Shaka, S.; Carpo, N.; Tran, V.; Ma, Y.-Y.; Karouia, F.; Espinosa-Jeffrey, A. Human Neural Stem Cells in Space Proliferate More than Ground Control Cells: Implications for Long-Term Space Travel. *Stem Cell Research* **2021**, *7*, 69. https://doi.org/10.24966/SRDT-2060/100069.
5. Kroemer, G.; Levine, B. Autophagic Cell Death: The Story of a Misnomer. *Nat. Rev. Mol. Cell Biol.* **2008**, *9*, 1004–1010. https://doi.org/10.1038/nrm2527.
6. Alkabie, S.; Basivireddy, J.; Zhou, L.; Roskams, J.; Rieckmann, P.; Quandt, J.A. SPARC Expression by Cerebral Microvascular Endothelial Cells in Vitro and Its Influence on Blood-Brain Barrier Properties. *J. Neuroinflammation* **2016**, *13*, 225. https://doi.org/10.1186/s12974-016-0657-9.

7. Bradshaw, A.D. The Role of SPARC in Extracellular Matrix Assembly. *J. Cell Commun. Signal.* **2009**, *3*, 239–246. https://doi.org/10.1007/s12079-009-0062-6.
8. Denton, D.; Kumar, S. Autophagy-Dependent Cell Death. *Cell Death Differ.* **2019**, *26*, 605–616. https://doi.org/10.1038/s41418-018-0252-y.
9. Nagaraju, G.P.; Dontula, R.; El-Rayes, B.F.; Lakka, S.S. Molecular Mechanisms Underlying the Divergent Roles of SPARC in Human Carcinogenesis. *Carcinogenesis* **2014**, *35*, 967–973. https://doi.org/10.1093/carcin/bgu072.
10. Espinosa-Jeffrey, A.; Becker-Catania, S.; Zhao, P.M.; Cole, R.; de Vellis, J. Phenotype Specification and Development of Oligodendrocytes and Neurons from Rat Stem Cell Cultures Using Two Chemically Defined Media. *J. Neurosci. Res.* **2002**, *69*, 810-825.
11. Espinosa-Jeffrey, A.; Wakeman, D.R.; Kim, S.U.; Snyder, E.Y.; de Vellis, J. Culture System for Rodent and Human Oligodendrocyte Specification, Lineage Progression, and Maturation. *Current Protocols in Stem Cell Biology* **2009**, *10*, 2D.4.1-2D.4.26. https://doi.org/10.1002/9780470151808.sc02d04s10.
12. Espinosa-Jeffrey, A.; Blanchi, B.; Biancotti, J.C.; Kumar, S.; Hirose, M.; Mandefro, B.; Talavera-Adame, D.; Benvenisty, N.; de Vellis, J. Efficient Generation of Viral and Integration-Free Human Induced Pluripotent Stem Cell-Derived Oligodendrocytes. *Current Protocols in Stem Cell Biology* **2016**, *38*, 2D.18.1-2D.18.27. https://doi.org/10.1002/cpsc.11.
13. Shaka, S.; Carpo, N.; Tran, V.; Espinosa-Jeffrey, A. Behavior of Astrocytes Derived from Human Neural Stem Cells Flown onto Space and Their Progenies. *Applied Sciences* **2021**, *11*, 41. https://doi.org/10.3390/app11010041.
14. Biancotti, J.C.; Carpo, N.; Zamudio, J.; Vergnes, L.; Espinosa-Jeffrey, A. Profiling the Secretome of Space Traveler Human Neural Stem Cells. *HSOA J. Stem Cells Res. Dev.* **2022**, 8, 1–12. https://doi.org/10.24966/SRDT-2060/100094.
15. Laggner, M.; Pollreisz, A.; Schmidinger, G.; Schmidt-Erfurth, U.; Chen, Y.-T. Autophagy Mediates Cell Cycle Response by Regulating Nucleocytoplasmic Transport of PAX6 in Limbal Stem Cells under Ultraviolet-A Stress. *PLOS ONE* **2017**, *12*, e0180868. https://doi.org/10.1371/journal.pone.0180868.
16. Wang, M.-M.; Feng, Y.-S.; Yang, S.-D.; Xing, Y.; Zhang, J.; Dong, F.; Zhang, F. The Relationship Between Autophagy and Brain Plasticity in Neurological Diseases. Fron*tiers in Cellular Neuroscience* **2019**, *13*.
17. Ohsumi, Y. Molecular Dissection of Autophagy: Two Ubiquitin-like Systems. *Nat. Rev. Mol. Cell Biol.* **2001**, *2*, 211–216. https://doi.org/10.1038/35056522.
18. Ohsumi, T. Yoshinori Ohsumi: Autophagy from Beginning to End. Interview by Caitlin Sedwick. *J. Cell Biol.* **2012**, *197*, 164-165. https://doi.org/10.1083/jcb.1972pi.
19. Noda, T.; Ohsumi, Y. Tor, a Phosphatidylinositol Kinase Homologue, Controls Autophagy in Yeast. *Journal of Biological Chemistry* **1998**, *273*, 3963–3966. https://doi.org/10.1074/jbc.273.7.3963.
20. Sahu, R.; Kaushik, S.; Clement, C.C.; Cannizzo, E.S.; Scharf, B.; Follenzi, A.; Potolicchio, I.; Nieves, E.; Cuervo, A.M.; Santambrogio, L. Microautophagy of Cytosolic Proteins by Late Endosomes. *Dev. Cell* **2011**, *20*, 131-139. https://doi.org/10.1016/j.devcel.2010.12.003.
21. Li, W.-W.; Li, J.; Bao, J.-K. Microautophagy: Lesser-known Self-eating. *Cell Mol. Life Sci.* **2012**, *69*, 1125-1136. https://doi.org/10.1007/s00018-011-0865-5
22. Vincent, J.A.; Kwong, T.J.; Tsukiyama, T. ATP-Dependent Chromatin Remodeling Shapes the DNA Replication Landscape. *Nat. Struct. Mol. Biol.* **2008**, *15*, 477–484. https://doi.org/10.1038/nsmb.1419.
23. Funk, S.E.; Sage, E.H. The Ca2(+)-Binding Glycoprotein SPARC Modulates Cell Cycle Progression in Bovine Aortic Endothelial Cells. *Proceedings of the National Academy of Sciences* **1991**, *88*, 2648–2652. https://doi.org/10.1073/pnas.88.7.2648.
24. Funk, S.E.; Sage, E.H. Differential Effects of SPARC and Cationic SPARC Peptides on DNA Synthesis by Endothelial Cells and Fibroblasts. *Journal of Cellular Physiology* **1993**, *154*, 53–63. https://doi.org/10.1002/jcp.1041540108.
25. Sage, E.H. Terms of Attachment: SPARC and Tumorigenesis. *Nat. Med.* **1997**, *3*, 144–146. https://doi.org/10.1038/nm0297-144.
26. Vadlamuri, S.V.; Media, J.; Sankey, S.S.; Nakeff, A.; Divine, G.; Rempel, S.A. SPARC Affects Glioma Cell Growth Differently When Grown on Brain ECM Proteins in Vitro under Standard versus Reduced-Serum Stress Conditions. *Neuro-Oncology* **2003**, *5*, 244–254. https://doi.org/10.1093/neuonc/5.4.244.

27. Carrara, M.; Prischi, F.; Nowak, P.R.; Kopp, M.C.; Ali, M.M. Noncanonical Binding of BiP ATPase Domain to Ire1 and Perk Is Dissociated by Unfolded Protein CH1 to Initiate ER Stress Signaling. *eLife* **2015**, *4*, e03522. https://doi.org/10.7554/eLife.03522.
28. Sailaja, G.S.; Bhoopathi, P.; Gorantla, B.; Chetty, C.; Gogineni, V.R.; Velpula, K.K.; Gondi, C.S.; Rao, J.S. The Secreted Protein Acidic and Rich in Cysteine (SPARC) Induces Endoplasmic Reticulum Stress Leading to Autophagy-Mediated Apoptosis in Neuroblastoma. *International Journal of Oncology* **2013**, *42*, 188–196. https://doi.org/10.3892/ijo.2012.1678.
29. Chen, S.; Zou, Q.; Guo, Q.; Chen, Y.; Kuang, X.; Zhang, Y.; Liu, Y.; Wu, W.; Li, G.; Tu, L.; et al. SPARC Knockdown Reduces Glutamate-Induced HT22 Hippocampal Nerve Cell Damage by Regulating Autophagy. *Frontiers in Neuroscience* **2021**, *14*.
30. Bhoopathi, P.; Chetty, C.; Gujrati, M.; Dinh, D.H.; Rao, J.S.; Lakka, S. Cathepsin B Facilitates Autophagy-Mediated Apoptosis in SPARC Overexpressed Primitive Neuroectodermal Tumor Cells. *Cell Death Differ.* **2010**, *17*, 1529–1539. https://doi.org/10.1038/cdd.2010.28.
31. Pannuru, P.; Dontula, R.; Khan, A.A.; Herbert, E.; Ozer, H.; Chetty, C.; Lakka, S.S. MiR-Let-7f-1 Regulates SPARC Mediated Cisplatin Resistance in Medulloblastoma Cells. *Cellular Signalling* **2014**, *26*, 2193–2201. https://doi.org/10.1016/j.cellsig.2014.06.014.
32. Ma, J.; Ma, Y.; Chen, S.; Guo, S.; Hu, J.; Yue, T.; Zhang, J.; Zhu, J.; Wang, P.; Chen, G.; et al. SPARC Enhances 5-FU Chemosensitivity in Gastric Cancer by Modulating Epithelial-Mesenchymal Transition and Apoptosis. *Biochemical and Biophysical Research Communications* **2021**, *558*, 134–140. https://doi.org/10.1016/j.bbrc.2021.04.009.
33. Fenouille, N.; Robert, G.; Tichet, M.; Puissant, A.; Dufies, M.; Rocchi, S.; Ortonne, J.-P.; Deckert, M.; Ballotti, R.; Tartare-Deckert, S. The P53/P21Cip1/ Waf1 Pathway Mediates the Effects of SPARC on Melanoma Cell Cycle Progression. *Pigment Cell & Melanoma Research* **2011**, *24*, 219–232. https://doi.org/10.1111/j.1755-148X.2010.00790.x.
34. Tam, S.Y.; Wu, V.W.C.; Law, H.K.W. Influence of Autophagy on the Efficacy of Radiotherapy. *Radiat. Oncol.* **2017**, *12*, 57. https://doi.org/10.1186/s13014-017-0795-y.
35. Palumbo, S.; Pirtoli, L.; Tini, P.; Cevenini, G.; Calderaro, F.; Toscano, M.; Miracco, C.; Comincini, S. Different Involvement of Autophagy in Human Malignant Glioma Cell Lines Undergoing Irradiation and Temozolomide Combined Treatments. *Journal of Cellular Biochemistry* **2012**, *113*, 2308–2318. https://doi.org/10.1002/jcb.24102.
36. Schleicher, S.M.; Moretti, L.; Varki, V.; Lu, B. Progress in the Unraveling of the Endoplasmic Reticulum Stress/Autophagy Pathway and Cancer: Implications for Future Therapeutic Approaches. *Drug Resistance Updates* **2010**, *13*, 79–86. https://doi.org/10.1016/j.drup.2010.04.002.
37. Nagelkerke, A.; Bussink, J.; Geurts-Moespot, A.; Sweep, F.C.G.J.; Span, P.N. Therapeutic Targeting of Autophagy in Cancer. Part II: Pharmacological Modulation of Treatment-Induced Autophagy. *Seminars in Cancer Biology* **2015**, *31*, 99–105. https://doi.org/10.1016/j.semcancer.2014.06.001.
38. Wickman, G.; Julian, L.; Olson, M.F. How Apoptotic Cells Aid in the Removal of Their Own Cold Dead Bodies. *Cell Death Differ.* **2012**, *19*, 735-742.
39. Tran, V.; Carpo, N.; Cepeda, C.; Espinosa-Jeffrey, A. Oligodendrocyte Progenitors Display Enhanced Proliferation and Autophagy after Space Flight. *Biomolecules* **2023**, *13*, 201. https://doi.org/10.3390/biom13020201.